Scaling of fractal aggregates

Bayard K. Johnson, Robert F. Sekerka, and Michael P. Foley
Department of Physics, Carnegie Mellon University, Pittsburgh, Pennsylvania 15213
(Received 11 July 1994)

In this paper, we define flux, mass, density, and accumulation functions for the diffusion-limited aggregation (DLA) simulation. We assume time rescalings for each of these functions and for the radii that bring each of the graphs of these functions, separately, onto a curve that does not depend on time. We show, by comparison with DLA simulations in two and three dimensions, that this rescaling is appropriate. We use this rescaling to derive several partial differential equations involving the aforementioned functions, and to guide us in choosing analytic expressions that describe these functions.

PACS number(s): 05.70.Ln, 05.40.+j, 61.43.Bn, 61.43.Hv

I. INTRODUCTION

Many irreversible growth processes produce figures that are highly branched and complicated. A simulation that is believed to model many such physical systems is the diffusion-limited aggregation (DLA) simulation originated by Witten and Sander [1,2]. In the two-dimensional (2D) off-lattice DLA simulation, one releases a random walker (in our case, represented by a mathematical point) from the circumference of a large circle centered on a seed particle. If the walker returns to the circle, one starts another walker from the circle. If the walker comes within some designated capture distance r_c of the seed, it remains there, and another walker is released from the circle. This walker is again allowed to wander until it comes within r_c of either of the particles of the aggregate. This process continues until a predetermined size of the cluster has been achieved. This simulation has been used to model viscous fingering [3–10], crystal growth [5,11–13], electrochemical deposition [14–18], and the growth of bacterial colonies [19–22]. The similarity of the figures produced by the DLA simulation to these physical systems indicates that they have some aspects of their growth mechanisms in common. Since the probability that a walker lands on the boundary of the aggregate is proportional to the gradient of the solution to Laplace's equation, for which the potential takes on constant boundary values on the aggregate and on the circle, analysis of these simulations has involved treatment of fractal growth in terms of solutions to Laplace's equation [2,23].

One property that has received particular attention in the literature on growth and aggregation is the fractal dimension. Honda *et al.* [24,25] consider the way in which the "interior region" (the region that obeys the familiar fractal scaling of the aggregate) must evolve to derive a formula for the fractal dimension of DLA in any dimension greater than or equal to one. They make the assumption that growth continues at all radii for all times. Although we believe that this assumption is not appropriate for the DLA simulation, we feel that they take an insightful approach that warrants further development. In particular, they define a radial density profile that depends on time.

Plischke and Racz [26] developed the concept of the density profile and computed the rate of change of that function with number of particles. We will later define this rate to be the accumulation function. The active region, where the accumulation is nonzero, was considered. They showed that two characteristic lengths come into play (the width and the position of the maximum of the Gaussian shaped accumulation rate). We look deeper into the relationships between this and other distributions that characterize the DLA simulation.

We believe that an analytical expression for the radial density profile as a function of time t and distance r from the seed can be found. From this expression, one would not only obtain the fractal dimension of the aggregate, but also be able to determine the rate of accumulation at all radii.

II. DEFINITIONS

The mass function M is defined as the total number of aggregated particles within a radius r of the seed particle.

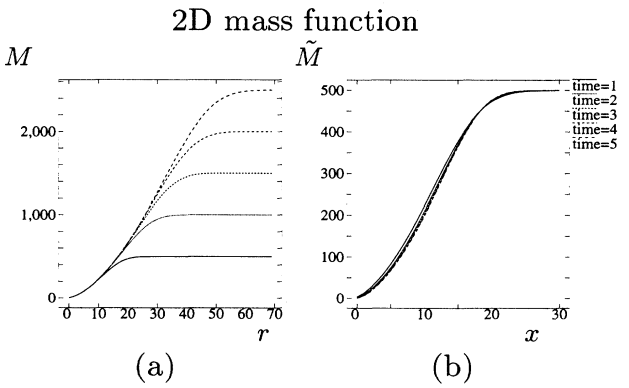

FIG. 1. 2D mass function for the DLA simulation. (a) is the simulated mass function M, computed by averaging 500 DLA figures. Each line represents an interval of 500 particles. The total number of walkers on each figure is 2500. (b) is obtained by rescaling the mass and radius with time.

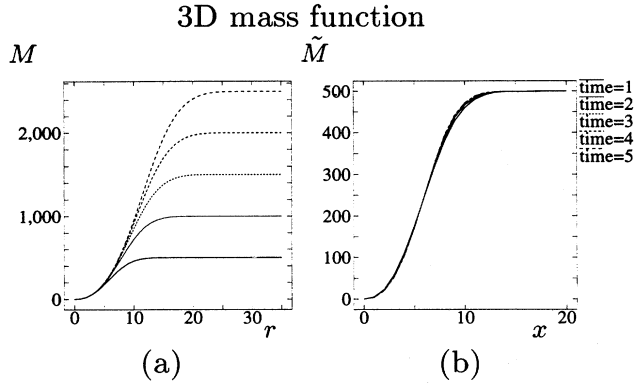

FIG. 2. 3D mass function for the DLA simulation. (a) is the simulated mass function M. (b) is obtained by rescaling the mass and radius with time.

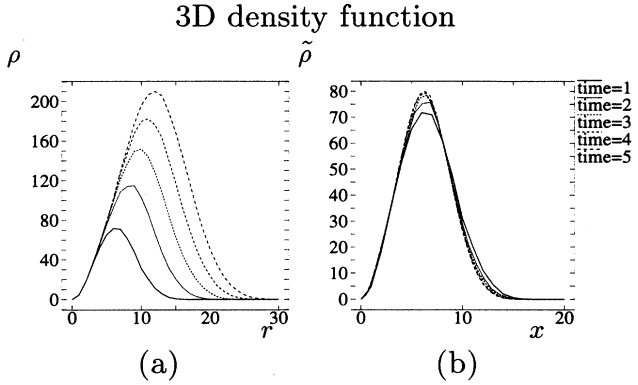

FIG. 4. 3D density function for the DLA simulation. (a) is the simulated density function ρ. (b) is obtained by rescaling the density and radius with time.

The radius r is a dimensionless variable measured in units of the capture distance r_c. The fractal dimension D of DLA that is most commonly computed is the slope of the $\ln(M)$ vs $\ln(r)$ plot for an aggregate which has been grown by the DLA algorithm. The fractal dimension for the DLA simulation has been determined from extremely large simulations to be approximately 1.71 [27] in two dimensions, and 2.49 [28] in three dimensions. For simplicity of discussion, we regard the definition of M to include dependence on a dimensionless (fictitious) "time" t by regarding each newly added particle to correspond to a fixed time interval Δt. Thus, $M(r,t)$ is defined as the number of particles on the aggregate which are within a radius r after $(t/\Delta t)$ particles have been added to the figure. $M(r,t)$ is shown for an actual DLA simulation in two dimensions in Fig. 1(a), and in three dimensions in Fig. 2(a) as a function of r for five different times. These figures and the next six, which result from actual DLA simulations, are based on the average of 500 two and three dimensional off-lattice DLA simulations at five time intervals corresponding to 500 particles per interval $(\Delta t = 1/500)$. Although t is a discrete variable, we assume that there is such a large number of added particles between observations that time can be treated as continuous.

The density function is defined in terms of M to be

$$\rho(r,t) := \frac{\partial M(r,t)}{\partial r} \ . \tag{1}$$

In other words, $\rho(r,t)dr$ is the number of particles contained within a shell between r and $r+dr$ at time t. This is shown for an actual DLA simulation in Fig. 3(a) and 4(a). The density function is simply Ω times the average density of accumulated particles at radius r, where $\Omega = 2\pi r$ in two dimensions, and $\Omega = 4\pi r^2$ in three. The flux function is defined to be

$$\Phi(r,t) := \frac{\partial M(r,t)}{\partial t} \ , \tag{2}$$

so that $\Phi(r,t)dt$ is the total number of particles that are accumulated within a circle of radius r in a time interval between t and $t+dt$. The function $\Phi(r,t)$ is plotted for actual DLA simulations in Fig. 5(a) and 6(a). Notice that the density function and the flux function can be related

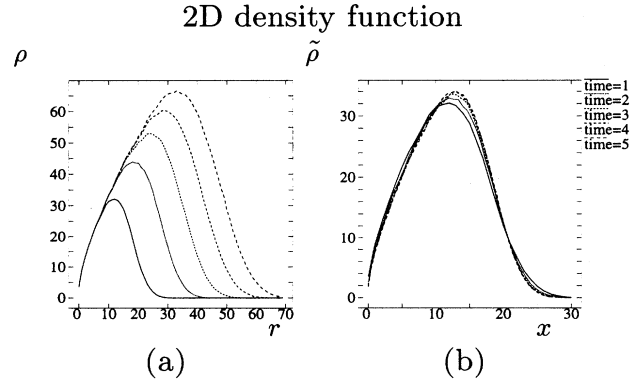

FIG. 3. 2D density function for the DLA simulation. (a) is the simulated density function ρ. (b) is obtained by rescaling the density and radius with time.

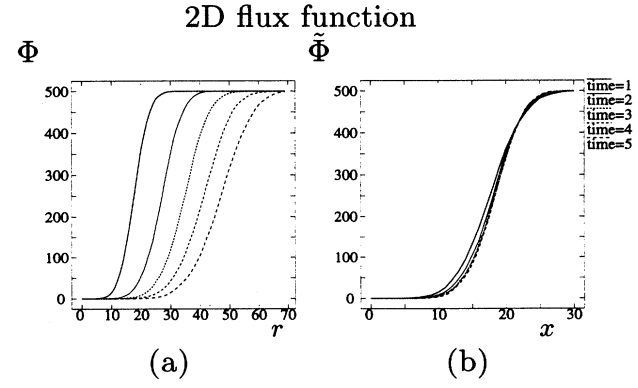

FIG. 5. 2D Flux function for the DLA simulation. (a) is the simulated flux function Φ. (b) is obtained by rescaling the radius with time.

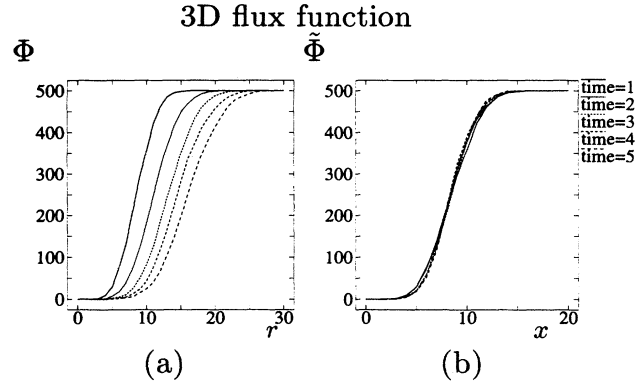

FIG. 6. 3D flux function for the DLA simulation. (a) is the simulated flux function Φ. (b) is obtained by rescaling the radius with time.

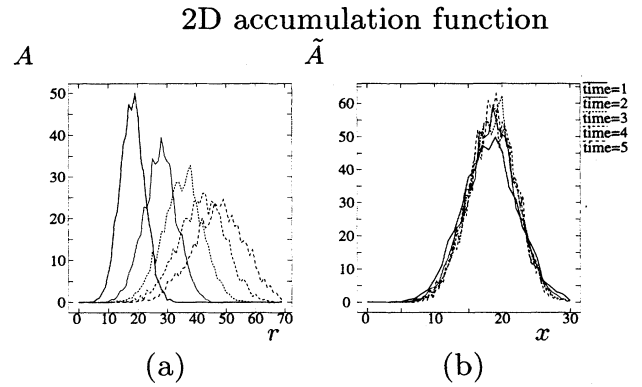

FIG. 7. 2D accumulation function for the DLA simulation. (a) is the simulated accumulation function A. (b) is obtained by rescaling the accumulation and radius with time.

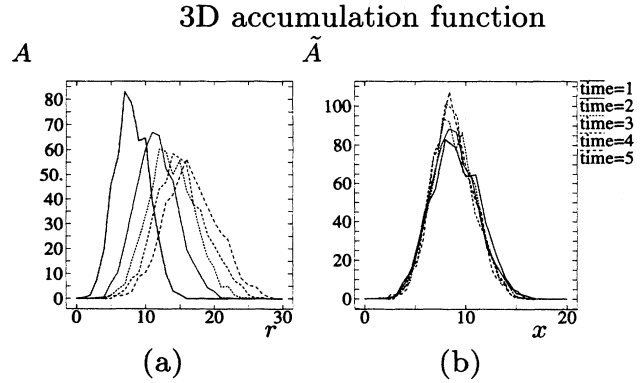

FIG. 8. 3D accumulation function for the DLA simulation. (a) is the simulated accumulation function A. (b) is obtained by rescaling the accumulation and radius with time.

through their derivatives:

$$\frac{\partial\rho(r,t)}{\partial t}=\frac{\partial\Phi(r,t)}{\partial r}\ . \tag{3}$$

Each of these derivatives is simply the mixed partial derivative of M with respect to r and t, which we define to be the accumulation function

$$A(r,t):=\frac{\partial^2 M}{\partial r\,\partial t}\ . \tag{4}$$

This is an expression for the rate of accumulation of particles at the distance r from the seed particle at time t. This quantity is plotted for actual simulations in Figs. 7(a) and 8(a). The function $A(r,t)$ is proportional to the probability that a walker which is released at time t lands on the figure at a distance r from the seed. A and Φ are obtained from time derivatives of ρ and M, respectively, and since ρ and M are determined from the instantaneous shape of the aggregate, A and Φ characterize the dynamics of the simulation.

III. RESCALED FUNCTIONS

For ease of discussion, we define three different regions of the growing cluster: the region inside the growing cluster that is shielded by the outer branches of the cluster and has essentially stopped growing is called the inert region; the portion of the cluster where nearly all of the growth occurs [where $A(r,t)\neq 0$] is called the active region; and the region outside of the maximum extent of the growing cluster is called the outer region.

We assume that we can rescale $M(r,t)$ and r with time t in such a way that the rescaled M, which we call $\tilde{M}(x)$, is independent of time. Since, in the outer region of the growing aggregate, M is increasing linearly with time, we must scale M by t. If we also assume that in the inert region $M\sim r^D$, where D is the fractal dimension of the figure, then $M/t\sim(r/t^{1/D})^D$, so we must scale r by $t^{1/D}$. We therefore define

$$\tilde{M}(x):=\frac{M(xt^{1/D},t)}{t} \tag{5a}$$

where $x=r/t^{1/D}$. We compare our expected rescaling with a rescaling of the actual simulation results, where we have chosen $D=1.71$ in two dimensions, and $D=2.49$ in three dimensions [28]. We plot $\tilde{M}$ in Figs. 1(b) and 2(b). Observe that M collapses to one curve upon rescaling. If we take derivatives of Eq. (5a) with respect to r and t, and extract the parts that are independent of time, we find rescalings for ρ, Φ, and A, each of which we expect to be independent of time:

$$\tilde{\rho}(x):=\frac{d\tilde{M}}{dx}=\rho(xt^{1/D},t)t^{1/D-1}\ , \tag{5b}$$

$$\tilde{\Phi}(x):=\tilde{M}-\frac{x}{D}\frac{d\tilde{M}}{dx}=\Phi(xt^{1/D},t)\ , \tag{5c}$$

$$\tilde{A}(x):=\frac{d\tilde{\Phi}}{dx}=A(xt^{1/D},t)t^{1/D}\ . \tag{5d}$$

The function $\tilde{\rho}$ is plotted in Figs. 3(b) and 4(b), $\tilde{\Phi}$ is plotted in Figs. 5(b) and 6(b) and $\tilde{A}$ is plotted in Figs. 7(b) and

8(b). Note that the first two plots in the figures for the DLA simulations do not align perfectly with the ones representing later times. We believe this is due to the fact that the initial condition, an isolated seed, is a great departure from the asymptotic behavior that occurs later. This initial condition gives rise to a transient that affects the data at early times. It can be argued that this departure signals multifractal behavior, but we contend that the data representing later times rescales appropriately.

IV. ANALYTICAL FORMS FOR THE FUNCTIONS

By substitution from Eq. (5), we find

$$M=\Phi t+\left\lfloor\frac{r}{D}\right\rfloor\rho\ . \tag{6}$$

By taking a derivative of Eq. (6) with respect to t and using Eq. (3), we obtain

$$\frac{\partial\Phi}{\partial t}=-\frac{r}{Dt}\frac{\partial\Phi}{\partial r}\ , \tag{7}$$

which is simply a first order linear homogenous partial differential equation for Φ. By the method of characteristics [29], the general solution of Eq. (7) is that Φ is an arbitrary function of $x=r/t^{1/D}$; in fact, by Eq. (5c) this function is just $\bar{\Phi}(x)$.

We know from the definition of Φ that it is constant in the outer region, and from the definition of the inert region, we know that Φ is essentially zero there. Therefore, to represent approximately the results of the simulations, we choose a function of x that is constant when x is large and is zero when x is small and undergoes a transition between the two regions; we then substitute the variable $r/t^{1/D}$ for the variable x in that function. An appropriate choice is

$$\Phi(r,t)=\frac{\Phi_\infty}{2}\left[1+\mathrm{erf}\left[\frac{(r/t^{1/D})-x_0}{\sqrt{2}\epsilon}\right]\right]\ , \tag{8}$$

where x_0, Φ , and ϵ are parameters, and erf(x) is the familiar error function [30]. Equation (8) is plotted in Fig. 9(a) for five different times. We have chosen $D=1.71$ for Fig. 9, corresponding to the two-dimensional case. Numerically integrating Eq. (8) with respect to t to obtain M, we produce the result shown in Fig. 9(b). We then determine ρ by substituting M and Φ into Eq. (6). The result is shown in Fig. 9(c). By taking a derivative of Eq. (8) with respect to r, the accumulation function becomes

$$A(r,t)=\frac{\Phi_\infty}{(2\pi\epsilon^2)^{1/2}t^{1/D}}\exp\left\{-\frac{[(r/t^{1/D})-x_0]^2}{2\epsilon^2}\right\}\ , \tag{9}$$

which is shown in Fig. 9(d). The Gaussian form for a fit to A was also used by Plischke and Racz in [26].

Note that the fractal dimension D that we used to plot these expressions was determined from analysis of an actual simulation in two dimensions, and not derived here. The analysis presented here is true in any integer dimension, provided we satisfy two assumptions: (1) there must exist a time rescaling of the functions that we introduced,

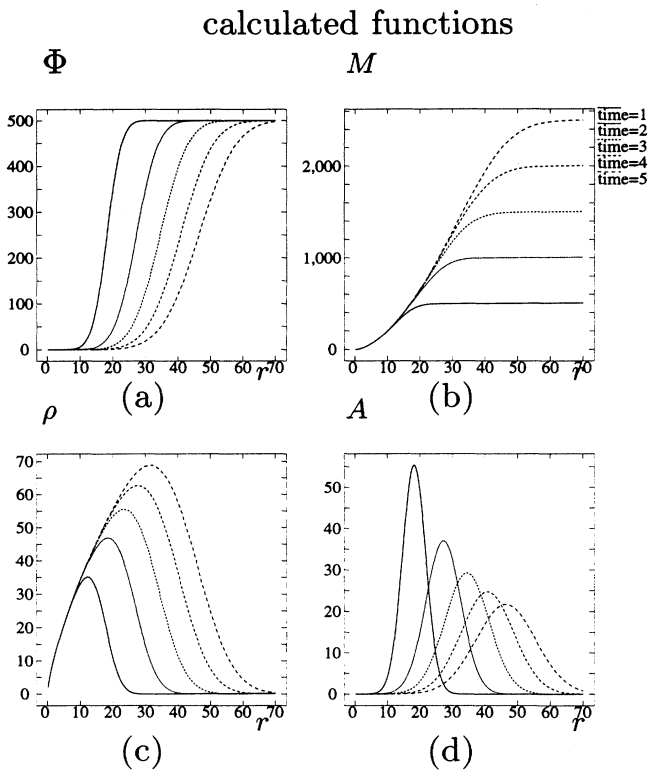

FIG. 9. Approximate functions for two dimensions. (a) is the calculated flux function that is determined from application of a rescaling to the definition of the flux function. (b) is the mass function, (c) the density function, and (d) the accumulation function. (a) is a best fit to an error function, [see Eq. (8)] and (b)–(d) are determined from Eqs. (5). The various lines correspond to five consecutive 500 particle intervals.

and (2) M must obey a power law dependence of the form $M\sim r^D$ in the inert region with D as a parameter.

V. INTERPRETATION OF THE ACCUMULATION FUNCTION

We now take a closer look at the accumulation function. Again, by manipulation of Eq. (5), we can write

$$A(r,t)=a\Phi\ , \tag{10}$$

in which

$$a:=\frac{\partial\ln\Phi}{\partial r}=\frac{\frac{\partial}{\partial r}[\rho/r^{D-1}]}{r\frac{\partial}{\partial r}[M/r^D]} \tag{11}$$

plays the role of an accumulation coefficient. The accumulation coefficient is the probability that a walker that wanders through the hypersphere of radius r actually sticks there. If one formulated a physical problem in such a way that the accumulation rate can be expressed in this way, then one could find a mapping between the DLA simulation and the physical system.

Observe that the accumulation coefficient does not depend explicitly on time, only implicitly through M and ρ. If we sought a nonlinear relationship between A and Φ, this would not be the case. M and ρ, as we mentioned before, characterize the static shape, and not the dynamics of the growth. If we stopped the simulation and examined the shape, we could compute a for that configuration. Substituting Eq. (6) into the definition of a we find

$$a=\frac{(D-1)\rho-r(\partial\rho/\partial r)}{DM-r\rho} . \tag{12}$$

If one carefully considers the DLA simulation algorithm, one can interpret this expression for a in terms of the number of sites available for attachment at radius r. The first term in the numerator is proportional to the total number of sites at radius r that belong to the aggregate. To determine the total number of sites available for attachment, we must subtract the second term in the numerator. This term accounts for the occupied sites that are just outside of those at radius r and that shield the sticking sites at r. The denominator is simply the integral from 0 to r of the numerator. The denominator normalizes a with respect to the total number of landing sites *within* r. For example, imagine very few landing sites on the aggregate inside of r. Then a would have to be correspondingly large, since Φ is defined as the total rate at which particles land within radius r. The fact that Φ and a are defined in terms of properties of the growing aggregate *within* r has an interpretation in which Φ is analogous to an electrostatic flux on a shell of radius r.

Borrowing from electrostatics, we can imagine the aggregate to be a perfect conductor that is held at a potential that differs from that of the starting circle. The flux function $\Phi(r,t)$ is proportional to the total electrostatic flux passing through a circular shell located at radius r, and is therefore proportional to the total charge contained within that shell, which is known from Gauss' law. Continuing with this analogy, $A\,dr$ is directly proportional to the amount of charge on the conducting aggregate that resides on a shell of thickness dr at a distance r from the seed. Since the interior of the aggregate is shielded by the branches from any potential gradients, one finds that there is no "charge" on the surface of the aggregate in the interior region.

V. DISCUSSION

The goal of much of the research in the study of figures produced from the DLA simulation is to determine the value of the fractal dimension D. To do this, one must account for the dynamical processes of random walk and for the interaction of these processes with the boundary of a complex aggregate. The mass and density functions are determined from the instantaneous shape of the aggregate, and the flux and accumulation functions are determined from the dynamics of the simulation. Equation (10) decomposes the accumulation rate into the product of two parts: a, which is influenced only by the instantaneous shape of the aggregate, and Φ which can be related to the dynamical processes which provide the evolution of the aggregate. By introducing the flux function, we provide the machinery to isolate the dynamics of the simulation, and to draw a clear electrostatic analog. We hope that this work will provide some of the tools necessary to more thoroughly understand the complex processes involved in fractal growth.

ACKNOWLEDGMENTS

The authors would like to acknowledge helpful discussions with Priyantha Perera. Financial support for this project has been provided by the National Science Foundation, Division of Materials Research under Grant No. DMR-9211276. Some computing resources have been provided by Pittsburgh Supercomputing Center under Grant No. DMR-890013P.

[1] T. A. Witten and L. M. Sander, Phys. Rev. Lett. **47**, 1400 (1981).
[2] T. A. Witten and L. M. Sander, Phys. Rev. B **27**, 5686 (1983).
[3] A. Arneodo *et al.* Phys. Rev. Lett. **63**, 984 (1989).
[4] G. Daccord, J. Nittmann, and H. E. Stanley, Phys. Rev. Lett. **56**, 336 (1986).
[5] H. Stanley, Physica A **163**, 334 (1990).
[6] J. F. Fernandez and J. M. Albarran, Phys. Rev. Lett. **64**, 2133 (1990).
[7] J. Nittmann, G. Daccord, and H. E. Stanley, Nature **314**, 141 (1985).
[8] S. Liang, Phys. Rev. A **33**, 2663 (1986).
[9] E. Ben-Jacob *et al.*, Phys. Rev. Lett. **57**, 1903 (1986).
[10] F. Family and T. Vicsek, Comput. Phys. **4**, 44 (1990).
[11] J. Nittmann and H. E. Stanley, J. Phys. A **20**, L981 (1987)
[12] T. Vicsek, Phys. Rev. Lett. **53**, 2281 (1984).
[13] T. Vicsek, Phys. Rev. A **32**, 3084 (1985).
[14] E. Ben-Jacob and P. Garik, Nature **343**, 523 (1990).
[15] P. Wynblatt, J. J. Metois, and J. C. Heyraud, J. Cryst. Growth **102**, 618 (1990).
[16] P. Garik *et al.*, Phys. Rev. Lett. **57**, 2703 (1989).
[17] R. M. Brady and R. C . Ball, Nature **309**, 225 (1984).
[18] M. Matsushita *et al.*, Phys. Rev. Lett. **53**, 286 (1984).
[19] E. Ben-Jacob *et al.*, Physica A **187**, 378 (1992).
[20] H. Fujikawa and M. Matsushita, J. Phys. Soc. Jpn. **58**, 3875 (1989).
[21] H. Fujikawa and M. Matsushita J. Phys. Soc. Jpn. **60**, 88 (1991).
[22] M. Matsushita and H. Fujikawa Physica A **168**,498 (1990).
[23] J. Lee, A. Coniglio, and H. E. Stanley, Phys. Rev. A **41**, 4589 (1990).
[24] K. Honda *et al.*, J. Phys. Soc. Jpn. **55**, 707 (1986).
[25] K. Honda, H. Toyoki, and M. Matsushita, J. Phys. Soc. Jpn. **55**, 2618 (1986).
[26] M. Plischke and R. Racz, Phys. Rev. Lett. **53**, 415 (1984).
[27] P. Meakin *et al.*, Rev. A **34**, 3325 (1986).
[28] T. C. Halsey and M. Leibig, Phys. Rev. A **46**, 7793 (1992).
[29] F. B. Hildebrand, *Advanced Calculus for Applications* (Prentice-Hall, Englewood Cliffs, NJ, 1962).
[30] *Handbook of Mathematical Functions,* Natl. Bur. Stand. Appl. Math. Ser. No. 55, edited by M. Abramowitz and I. A. Stegun (U.S. GPO, Washington D.C., 1964).